arXiv:physics/0102070v1 [physics.atom-ph] 22 Feb 2001

,

High-precision calculations of electric-dipole amplitudes for transitions between low-lying levels of Mg, Ca, and Sr

S. G. Porsev,* M. G. Kozlov, and Yu. G. Rakhlina

Petersburg Nuclear Physics Institute,
Gatchina, Leningrad district, 188300, Russia

A. Derevianko

Physics Department, University of Nevada, Reno, Nevada 89557

(Dated: February 2, 2008)

Abstract

To support efforts on cooling and trapping of alkaline-earth atoms and designs of atomic clocks, we performed *ab initio* relativistic many-body calculations of electric-dipole transition amplitudes between low-lying states of Mg, Ca, and Sr. In particular, we report amplitudes for $^1P_1^o \to {}^1S_0, {}^3S_1, {}^1D_2$, for $^3P_1^o \to {}^1S_0, {}^1D_2$, and for $^3P_2^o \to {}^1D_2$ transitions. For Ca, the reduced matrix element $\langle 4s4p\,{}^1P_1^o||D||4s^2\,{}^1S_0\rangle$ is in a good agreement with a high-precision experimental value deduced from photoassociation spectroscopy [Zinner *et al.*, Phys. Rev. Lett. **85**, 2292 (2000)]. An estimated uncertainty of the calculated lifetime of the $3s3p\,{}^1P_1^o$ state of Mg is a factor of three smaller than that of the most accurate experiment. Calculated binding energies reproduce experimental values within 0.1-0.2%.

PACS numbers: 31.10.+z, 31.15.Ar, 31.15.Md, 32.70.Cs

---

*Electronic address: porsev@thd.pnpi.spb.ru

I. INTRODUCTION

Many-body methods have proven to be a highly accurate tool for determination of atomic properties, especially for systems with one valence electron outside a closed-shell core [1]. For alkali-metal atoms a comparison of highly-accurate experimental data with calculations [2] allows one to draw a conclusion that modern *ab initio* methods are capable of predicting basic properties of low-lying states with a precision better than 1%.

For *divalent* atoms such a comprehensive comparison was previously hindered by a lack of high-precision measurements of radiative lifetimes. Despite the lifetimes of the lowest $nsnp\,^1P_1^o$ and $nsnp\,^3P_1^o$ states were repeatedly obtained both experimentally and theoretically [3, 4, 5, 6, 7, 8, 9, 10, 11, 12, 13, 14, 15, 16, 17, 18, 19, 20, 21, 22, 23, 24], persistent discrepancies remain. Only very recently, Zinner *et al.* [3] have achieved 0.4% accuracy for the rate of $4s4p\,^1P_1^o \rightarrow 4s^2\,^1S_0$ transition in calcium. This high-precision value was deduced from photoassociation spectroscopy of ultracold calcium atoms. One of the purposes of the present work is to test the quality of many-body techniques for two-valence electron systems by comparing our result with the experimental value from Ref. [3].

We extend the earlier work [25] and report results of relativistic many-body calculation of energy levels and electric-dipole transition amplitudes for Mg, Ca and Sr. The calculations are performed in the framework of configuration-interaction approach coupled with many-body perturbation theory [26, 27]. We tabulate electric-dipole amplitudes for $^1P_1^o \rightarrow\, ^1S_0, ^3S_1, ^1D_2$, for $^3P_1^o \rightarrow\, ^1S_0, ^1D_2$, and for $^3P_2^o \rightarrow\, ^1D_2$ transitions and estimate theoretical uncertainties.

Cooling and trapping experiments with alkaline-earth atoms were recently reported for Mg [4], Ca [3, 29], and Sr [28, 30]. The prospects of achieving Bose-Einstein condensation were also discussed [3, 31]. Our accurate transition amplitudes will be helpful in designs of cooling schemes and atomic clocks. In addition, these amplitudes will aid in determination of long-range atomic interactions, required in calculation of scattering lengths and interpretation of cold-collision data. For example, dispersion (van der Waals) coefficient C_6 characterizes the leading dipole-dipole interaction of two ground-state atoms at large internuclear separations [32]. The coefficient C_6 is expressed in terms of energy separations and electric-dipole matrix elements between the ground and excited atomic states. Approximately 80% of the total value of C_6 arises from the principal transition $nsnp\,^1P_1^o - ns^2\,^1S_0$, requiring accurate predictions for the relevant matrix element. Therefore our results will be also useful in determination of dispersion coefficients.

II. METHOD OF CALCULATIONS

In atomic-structure calculations, correlations are conventionally separated into three classes: valence-valence, core-valence, and core-core correlations. A strong repulsion of valence electrons has to be treated non-perturbatively, while it is impractical to handle the two other classes of correlations with non-perturbative techniques, such as configuration-interaction (CI) method. Therefore, it is natural to combine many-body perturbation theory (MBPT) with one of the non-perturbative methods. It was suggested [26] to use MBPT to construct an effective Hamiltonian $H_{\rm eff}$ defined in the model space of valence electrons. Energies and wavefunctions of low-lying states are subsequently determined using CI approach, i.e. diagonalizing $H_{\rm eff}$ in the valence subspace. Atomic observables are calculated with effective operators [27]. Following the earlier work, we refer to this method as CI+MBPT formalism.

In the CI+MBPT approach the energies and wavefunctions are determined from the Schrödinger equation

$$H_{\rm eff}(E_n)\,|\Phi_n\rangle = E_n\,|\Phi_n\rangle\,, \tag{1}$$

where the effective Hamiltonian is defined as

$$H_{\rm eff}(E) = H_{\rm FC} + \Sigma(E). \tag{2}$$

Here $H_{\rm FC}$ is the two-electron Hamiltonian in the frozen core approximation and Σ is the energy-dependent correction, involving core excitations. The operator Σ completely accounts for the second order of perturbation theory. Determination of the second order corrections requires calculation of one– and two–electron diagrams. The one–electron diagrams describe an attraction of a valence electron by a (self-)induced core polarization. The two-electron diagrams are specific for atoms with several valence electrons and represent an interaction of a valence electron with core polarization induced by another valence electron.

Already at the second order the number of the two–electron diagrams is large and their computation is very time-consuming. In the higher orders the calculation of two-electron diagrams becomes impractical. Therefore we account for the higher orders of MBPT indirectly. It was demonstrated [33] that a proper approximation for the effective Hamiltonian can substantially improve an agreement between calculated and experimental spectra of multielectron atom. One can introduce an energy shift δ and replace $\Sigma(E) \rightarrow \Sigma(E-\delta)$ in the effective Hamiltonian, Eq. (2). The choice δ=0 corresponds to the Brillouin-Wigner variant of MBPT and the Rayleigh-Schrödinger variant is recovered setting $\delta = E_n - E_n^{(0)}$, where $E_n^{(0)}$ is the zero-order energy of level n. The latter is more adequate for multielectron systems [34]; for few-electron systems an intermediate value of δ is optimal. We have determined δ from a fit of theoretical energy levels to experimental spectrum. Such an optimized effective Hamiltonian was used in calculations of transition amplitudes.

To obtain an effective electric-dipole operator we solved random-phase approximation (RPA) equations, thus summing a certain sequence of many-body diagrams to all orders of MBPT. The RPA describes a shielding of externally applied field by core electrons. We further incorporated one- and two-electron corrections to the RPA to account for a difference between the V^N and V^{N-2} potentials and for the Pauli exclusion principle. In addition, the effective operator included corrections for normalization and structural radiation [27]. The RPA equations depend on transition frequency and should be solved independently for each transition. However, the frequency dependence was found to be rather weak and we solved these equations only at some characteristic frequencies. To monitor a consistency of the calculations we employed both length (L) and velocity (V) gauges for the electric-dipole operator.

The computational procedure is similar to calculations of hyperfine structure constants and electric-dipole amplitudes for atomic ytterbium [35, 36]. We consider Mg, Ca and Sr as atoms with two valence electrons above closed cores [$1s$,...,$2p^6$], [$1s$,...,$3p^6$], and [$1s$,...,$4p^6$], respectively [37]. One-electron basis set for Mg included $1s$–$13s$, $2p$–$13p$, $3d$–$12d$, and $4f$–$11f$ orbitals, where the core- and 3,4s, 3,4p, 3,4d, and 4f orbitals were Dirac-Hartree-Fock (DHF) ones, while all the rest were virtual orbitals. The orbitals $1s$–$3s$ were constructed by solving the DHF equations in V^N approximation, $3p$ orbitals were obtained in the V^{N-1} approximation, and $4s$, $4p$, 3,4d, and $4f$ orbitals were constructed in the V^{N-2} approximation. We determined virtual orbitals using a recurrent procedure, similar to Ref. [38] and employed in previous work [26, 27, 35, 36]. The one-electron basis set for Ca included $1s$–$13s$, $2p$–$13p$,

$3d$–$12d$, and $4f$–$11f$ orbitals, where the core- and $4s$, $4p$, and $3d$ orbitals are DHF ones, while the remaining orbitals are the virtual orbitals. The orbitals $1s$–$4s$ were constructed by solving the DHF equations in the V^N approximation, and $4p$ and $3d$ orbitals were obtained in the V^{N-1} approximation. Finally, the one-electron basis set for Sr included $1s$–$14s$, $2p$–$14p$, $3d$–$13d$, and $4f$–$13f$ orbitals, where the core- and $5s$, $5p$, and $4d$ orbitals are DHF ones, and all the rest are the virtual orbitals. The orbitals $1s$–$5s$ were constructed by solving the DHF equations in the V^N approximation, and $5p$ and $4d$ orbitals were obtained in the V^{N-1} approximation. Configuration-interaction states were formed using these one-particle basis sets. It is worth emphasizing that the employed basis sets were sufficiently large to obtain numerically converged CI results. A numerical solution of random-phase approximation equations required an increase in the number of virtual orbitals. Such extended basis sets included $1s$–ks, $2p$–kp, $3d$–$(k\text{-}1)d$, $4f$–$(k\text{-}4)f$, and $5g$–$(k\text{-}8)g$ orbitals, where k=19,20,21 for Mg, Ca, and Sr, respectively. Excitations from all core shells were included in the RPA setup.

III. RESULTS AND DISCUSSION

A. Energy levels

In Tables I – III we present calculated energies of low-lying states for Mg, Ca, and Sr and compare them with experimental values. The two-electron binding energies were obtained both in the framework of conventional configuration-interaction method and using the formalism of CI coupled with many-body perturbation theory. Already at the CI stage the agreement of the calculated and experimental energies is at the level of 5%. The addition of many-body corrections to the Hamiltonian improves the accuracy by approximately an order of magnitude. Finally, with an optimal choice of parameter δ the agreement with experimental values improves to 0.1–0.2%.

Compared to the binding energies, fine-structure splitting of triplet states and singlet-triplet energy differences represent a more stringent test of our method. For the $^3P^o_{1,2,3}$-states the fine-structure splitting is reproduced with an accuracy of several per cent in the pure CI for all the three atoms, while the $^3P^o_1$ – $^1P^o_1$ energy differences are less accurate (especially for Ca and Sr). As demonstrated in Ref. [33], the two-electron exchange Coulomb integral $R_{np,ns,ns,np}$ (n=3,4,5 for Mg, Ca, and Sr, respectively) determining the splitting between $^3P^o_1$ and $^1P^o_1$ states is very sensitive to many-body corrections. Indeed, with these corrections included, the agreement with the experimental data improves to 1-2% for all the three atoms.

The case of the even-parity $^{3,1}D_J$-states is even more challenging. For Ca, these four states are practically degenerate at the CI stage. A repulsion of the level $^1D_2$ from the upper-lying levels of np^2 configuration pushes it down to the level $^3D_2$ and causes their strong mixing. As seen from Table II these states are separated only by 10 cm^{-1}, while the experimental energy difference is 1550 cm^{-1}. As a result, an accurate description of superposition of $^3D_2$ and $^1D_2$ states is important. The $^3D_2$ – $^1D_2$ splitting is restored when the many-body corrections are included in the effective Hamiltonian. These corrections properly account for core polarization screening an interaction between sd and p^2 configurations.

For Sr, the fine-structure splittings of ^3D_J states and energy difference between the ^3D_J and the $^1D_2$ levels are also strongly underestimated in the pure CI method. Again the inclusion of the many-body corrections substantially improves the splittings between the D-states. It is worth emphasizing, that for such an accurate analysis a number of effects was taken into account, i.e., spin-orbit interaction, configuration interaction, and core-valence correlations. A proper account for all these effects is of particular importance for determination of electric-dipole amplitudes forbidden in LS-coupling, such as for ${}^3P^o_J \rightarrow {}^1S_0, {}^1D_2$ transitions.

B. Transition amplitudes

In this section we present calculations of electric-dipole (E1) amplitudes for ${}^{3,1}P^o_1 \rightarrow {}^1S_0$, ${}^{3,1}P^o_1 \rightarrow {}^1D_2$, ${}^3P^o_2 \rightarrow {}^1D_2$, and ${}^1P^o_1 \rightarrow {}^3S_1$ transitions. The calculated reduced matrix elements for Mg, Ca, and Sr are presented in Tables IV and V. For a transition $I \rightarrow F$ the Einstein rate coefficients for spontaneous emission (in $1/s$) are expressed in terms of these reduced matrix elements $\langle F||D||I\rangle$ (a.u.) and wavelengths λ (Å) as

$$A_{FI} = \frac{2.02613 \times 10^{18}}{\lambda^3} \frac{|\langle F||D||I\rangle|^2}{2J_I + 1} \,. \tag{3}$$

A number of long-range atom-atom interaction coefficients could be directly obtained from the calculated matrix elements. At large internuclear separations R an atom in a state $|A\rangle$ predominantly interacts with a like atom in a state $|B\rangle$ through a potential $V(R) \approx \pm C_3/R^3$, provided an electric-dipole transition between the two atomic states $|A\rangle$ and $|B\rangle$ is allowed. The coefficient C_3 is given by

$$|C_3| = |\langle A||D||B\rangle|^2 \sum_{\mu=-1}^{1} (1 + \delta_{\mu,0}) \begin{pmatrix} J_A & 1 & J_B \\ -\frac{\Omega+\mu}{2} & \mu & \frac{\Omega-\mu}{2} \end{pmatrix}^2 , \tag{4}$$

where Ω is the conventionally defined sum of projections of total angular momenta on internuclear axis.

From a solution of the eigen-value problem, Eq. (1), we obtained wave functions, constructed effective dipole operators, and determined the transition amplitudes. The calculations were performed within both traditional configuration-interaction method and CI coupled with the many-body perturbation theory. The comparison of the CI and the CI+MBPT values allows us to estimate an accuracy of our calculations. As it was mentioned above, to monitor the consistency of the calculations, we determined the amplitudes using both length and velocity gauges for the dipole operator. In general, dipole amplitudes calculated in the velocity gauge are more sensitive to many-body corrections; we employ the length form of the dipole operator in our final tabulation.

We start the discussion with the amplitudes for the principal $nsnp\,{}^1P^o_1 \rightarrow ns^2\,{}^1S_0$ transitions ($n = 3$ for Mg, $n = 4$ for Ca, and $n = 5$ for Sr). Examination of Table IV reveals that the many-body effects reduce the L-gauge amplitudes by 1.6% for Mg, 5.5% for Ca, and 6.4% for Sr. Further, the MBPT corrections bring the length and velocity-form results into a closer agreement. For example, for Sr at the CI level the velocity and length forms differ by 2.7% and this discrepancy is reduced to 0.8% in the CI+MBPT calculations.

A dominant theoretical uncertainty of the employed CI+MBPT method is due to impossibility to account for all the orders of many-body perturbation theory. It is worth emphasizing that in our CI calculations the basis sets were saturated and the associated numerical errors were negligible. We expect that the theoretical uncertainty is proportional to the determined many-body correction. In addition, we take into account the proximity of the amplitudes obtained in the L- and V-gauges. We estimate the uncertainties for the

$nsnp\,^1P_1^o \rightarrow ns^2\,^1S_0$ transition amplitudes as 25–30% of the many-body corrections in the length gauge. The final values for $\langle nsnp\,^1P_1^o||D||ns^2\,^1S_0\rangle$, recommended from the present work, are 4.03(2) for Mg, 4.91(7) for Ca, and 5.28(9) a.u. for Sr.

We present a comparison of our results for $\langle nsnp\,^1P_1^o||D||ns^2\,^1S_0\rangle$ with experimental data in Table IV and in Fig. 1. Our estimated accuracy for Mg is a factor of three better than that of the most accurate experiment and for Sr is comparable to experimental precision. For Ca, the dipole matrix element of the $^1P_1^o \rightarrow {}^1S_0$ was recently determined with a precision of 0.2% by Zinner *et al.* [3] using photoassociation spectroscopy of ultracold Ca atoms. While our result is in harmony with their value, the experimental accuracy is substantially better. An updated analysis [40] of photoassociation spectra of Ref. [3] leads to a somewhat better agreement with our calculated value.

A very extensive compilation of earlier theoretical results for the $^1P_1^o \rightarrow {}^1S_0$ transition amplitudes can be found in Ref. [6] for Mg and in Ref. [9] for Ca. In a very recent multiconfiguration Hartree-Fock (MCHF) calculations for Mg [7] the authors have determined $\langle 3s3p\,^1P_1^o||D||3s^2\,^1S_0\rangle = 4.008$ a.u. This value agrees with our final result of 4.03(2) a.u. For heavier Sr the correlation effects are especially pronounced and only a few calculations were performed. For example, MCHF calculations for Sr [8] found in the length gauge $\langle 5s5p\,^1P_1^o||D||5s^2\,^1S_0\rangle = 5.67$ a.u. By contrast to the present work, the core-polarization effects were not included in this analysis. As a result, this calculated value is in a good agreement with our result 5.63 a.u. obtained at the CI stage, but differs from the final value 5.28(9) a.u.

Another nonrelativistically allowed transition is $^1P_1^o \rightarrow {}^1D_2$ and one could expect that this amplitude can be determined with a good accuracy. For Mg this is really so. However, for Ca and Sr an admixture of the configuration p^2 brings about large corrections to this amplitude, especially in the velocity gauge. Another complication is the following. The matrix element of electric-dipole operator can be represented in the V-gauge as (atomic units $\hbar = |e| = m_e = 1$ are used):

$$\langle F|\mathbf{D}|I\rangle = i\,c\,\langle F|\boldsymbol{\alpha}|I\rangle/(E_I - E_F). \tag{5}$$

Here c is the speed of light, E_I and E_F are the energies of initial and final states, and $\boldsymbol{\alpha}$ are the Dirac matrices. For the $^1P_1^o \rightarrow {}^1D_2$ transition in Ca and Sr the energy denominator is approximately 0.01 a.u. Because the E1-amplitudes of these transitions ~ 1 a.u. (see Table IV), the respective numerators are of the order of 0.01 a.u. Correspondingly the matrix elements $\langle F|\boldsymbol{\alpha}|I\rangle$ are small and are very sensitive to corrections, i.e., the V-gauge results are unstable. As a result we present only the L-gauge values for $^1P_1^o \rightarrow {}^1D_2$ E1 amplitudes for Ca and Sr. An absence of reliable results in V-gauge hampers an estimate of the accuracy, so we rather conservatively take it to be 25%. Note that even with such a large uncertainty our value for Sr significantly differs from the experimental value [24]. The measurement in [24] has been carried out on the $^1D_2 \rightarrow {}^1S_0$ transition and an interference between electric-quadrupole (E2) and Stark-induced dipole amplitudes was observed. In order to determine the transition rate a theoretical value of the E2-amplitude for the $^1D_2 \rightarrow {}^1S_0$ transition was taken from [41]. It may be beneficial either to measure directly the rate of the E1-transition $^1P_1^o \rightarrow {}^1D_2$ or to measure the rate of the E2-transition $^1D_2 \rightarrow {}^1S_0$.

For the $^3P_J^o \rightarrow {}^1S_0, {}^1D_2$ transitions the respective E1-amplitudes are small; these are nonrelativistically forbidden intercombination transitions and consequently their amplitudes are proportional to spin-orbit interaction. The calculated reduced matrix elements are presented in Table V.

One can see from Tables I – III that the MBPT corrections to the fine structure splittings are large, amplifying significance of higher order many-body corrections. In addition, higher order corrections in the fine-structure constant α to the Dirac-Coulomb Hamiltonian are also important here. As demonstrated in Ref. [6], the Breit interaction reduces the dipole amplitude of ${}^3P_1^o \rightarrow {}^1S_0$ transition in Mg by 5%. At the same time for all the intercombination transitions the agreement between L- and V-gauges is at the level of 6-8%. We conservatively estimate the uncertainties of the calculated intercombination E1 amplitudes to be 10–12%.

To reiterate, we carried out calculations of energies of low-lying levels and electric-dipole amplitudes between them for divalent atoms Mg, Ca, and Sr. We employed *ab initio* relativistic configuration interaction method coupled with many-body perturbation theory. The calculated removal energies reproduce experimental values within 0.1-0.2%. A special emphasis has been put on accurate determination of electric-dipole amplitudes for principal transitions $nsnp\,{}^1P_1^o \rightarrow ns^2\,{}^1S_0$. For these transitions, we estimated theoretical uncertainty to be 0.5% for Mg, 1.4% for Ca, and 1.7% for Sr. For Ca, the reduced matrix element $\langle 4s4p\,{}^1P_1^o||D||4s^2\,{}^1S_0\rangle$ is in a good agreement with a high-precision experimental value [3]. An estimated uncertainty of the calculated lifetime of the lowest ${}^1P_1^o$ state for Mg is a factor of three smaller than that of the most accurate experiment. In addition, we evaluated electric-dipole amplitudes and estimated theoretical uncertainties for ${}^1P_1^o \rightarrow {}^3S_1, {}^1D_2$, ${}^3P_1^o \rightarrow {}^1S_0, {}^1D_2$, and for ${}^3P_2^o \rightarrow {}^1D_2$ transitions. Our results could be useful in designs of cooling schemes and atomic clocks, and for accurate description of long-range atom-atom interactions needed in interpretation of cold-collision data.

Acknowledgments

We would like to thank H. Katori, C. Oates, and F. Riehle for stimulating discussions. This work was supported in part by the Russian Foundation for Basic Researches (grant No 98-02-17663). The work of A.D. was partially supported by the Chemical Sciences, Geosciences and Biosciences Division of the Office of Basic Energy Sciences, Office of Science, U.S. Department of Energy.

---

[1] J. Sapirstein, Rev. Mod. Phys. **70**, 55 (1998) and references therein.

[2] see, for example, M.S. Safronova, W.R. Johnson, and A. Derevianko, Phys. Rev. A **60**, 4476 (1999).

[3] G. Zinner, T. Binnewies, F. Riehle, and E. Tiemann, Phys. Rev. Lett. **85**, 2292 (2000).

[4] K. Sengstock, U. Sterr, G. Hennig, D. Bettermann, J.H. Muller, and W. Ertmer, Opt. Commun. **103**, 73 (1993).

[5] L. Liljeby, A. Lindgard, S. Mannervik, E. Veje, and B. Jelencovic, Phys. Scr. **21**, 805 (1980);

[6] P. Jönsson, and C. F. Fischer, J. Phys. B **30**, 5861 (1997).

[7] P. Jönsson, C.F. Fischer, and M.R. Godefroid, J. Phys. B **32**, 1233 (1999).

[8] N. Vaeck, M. Godefroid, and J.E. Hansen, Phys. Rev. A **38** 2830 (1988).

[9] T. Brage, C.F. Fischer, N. Vaeck, M. Godefroid, and A. Hibbert, Phys. Scr. **48**, 533 (1993) (and references therein).

TABLE I: Two-electron binding energies E_{val} in a.u. and energy differences Δ (cm^{-1}) for low-lying levels of Mg.

		CI		CI+MBPT		Experiment	
Config.	Level	E_{val}	Δ	E_{val}	Δ	E_{val}	Δ
$3s^2$	$^1S_0$	0.819907	—	0.833556	—	0.833518[a]	—
$3s\,4s$	$^3S_1$	0.635351	40505	0.645853	41196	0.645809	41197.4
$3s\,4s$	$^1S_0$	0.624990	42779	0.635283	43516	0.635303	43503.1
$3s\,3d$	$^1D_2$	0.613603	45278	0.621830	46469	0.622090	46403.1
$3s\,3p$	$^3P^o_0$	0.724170	21012	0.733896	21879	0.733961	21850.4
$3s\,3p$	$^3P^o_1$	0.724077	21032	0.733796	21901	0.733869	21870.4
$3s\,3p$	$^3P^o_2$	0.723889	21073	0.733596	21945	0.733684	21911.1
$3s\,3p$	$^1P^o_1$	0.662255	34601	0.674226	34975	0.673813	35051.4

[a] Two electron binding energy of the ground state is determined as a sum of the first two ionization potentials IP (Mg) and IP (Mg^+), where IP (Mg) = 61669.1 cm^{-1} and IP (Mg^+)= 121267.4 cm^{-1} [39].

TABLE II: Two-electron binding energies in a.u. and energy differences Δ in cm^{-1} for the low-lying levels of Ca.

		CI [a]		CI+MBPT		Experiment	
Config.	Level	E_{val}	Δ	E_{val}	Δ	E_{val}	Δ
$4s^2$	$^1S_0$	0.636590	—	0.661274	—	0.660927[b]	—
$4s\,3d$	$^3D_1$	0.528838	23649	0.567744	20527	0.568273	20335.3
$4s\,3d$	$^3D_2$	0.528868	23642	0.567656	20547	0.568209	20349.2
$4s\,3d$	$^3D_3$	0.528820	23653	0.567517	20577	0.568110	20371.0
$4s\,3d$	$^1D_2$	0.528824	23652	0.559734	22285	0.561373	21849.6
$4s\,5s$	$^3S_1$	0.498205	30372	0.517490	31557	0.517223	31539.5
$4s\,4p$	$^3P^o_0$	0.574168	13700	0.591521	15309	0.591863	15157.9
$4s\,4p$	$^3P^o_1$	0.573942	13750	0.591274	15363	0.591625	15210.1
$4s\,4p$	$^3P^o_2$	0.573486	13850	0.590774	15473	0.591143	15315.9
$4s\,4p$	$^1P^o_1$	0.530834	23211	0.553498	23654	0.553159	23652.3

[a] Note that the conventional CI fails to recover the correct ordering of *D*-states. [b] For the ground state E_{val}= IP (Ca)+IP (Ca^+), where IP (Ca) = 49304.8 cm^{-1} and IP (Ca^+) = 95752.2 cm^{-1} [39].

[10] H. G. C. Werij, C. H. Greene, C. E. Theodosiou and A. Gallagher, Phys. Rev. A **46**, 1248 (1992) (and references therein).

[11] F. M. Kelly and M. S. Mathur, Can. J. Phys. **58**, 1416 (1980).

[12] L. Lundin, B. Engman, J. Hilke, and I. Martinson, Phys. Scr. **8**, 274 (1973).

[13] W. H. Parkinson, E. M. Reeves, and F. S. Tomkins, J. Phys. B **9**, 157 (1976).

[14] W. W. Smith and A. Gallagher, Phys. Rev. A **145**, 26 (1966).

[15] W. J. Hansen, J. Phys. B **16**, 2309 (1983).

[16] A. Godone and C. Novero, Phys. Rev. A **45**, 1717 (1992).

[17] D. Husain and G. J. Roberts, J. Chem. Soc. Faraday Trans. 2 **82**, 1921 (1986).

[18] D. Husain and J. Schifino, J. Chem. Soc. Faraday Trans. 2 **80**, 321 (1984).

TABLE III: Two-electron binding energies in a.u. and energy differences Δ in cm^{-1} for the low-lying levels of Sr.

		CI		CI+MBPT		Experiment	
Config.	Level	$E_{\rm val}$	Δ	$E_{\rm val}$	Δ	$E_{\rm val}$	Δ
$5s^2$	$^1S_0$	0.586538	—	0.614409	—	0.614601[a]	—
$5s\,4d$	$^3D_1$	0.497148	19619	0.532110	18063	0.531862	18159.1
$5s\,4d$	$^3D_2$	0.497077	19635	0.531809	18129	0.531590	18218.8
$5s\,4d$	$^3D_3$	0.496941	19664	0.531298	18242	0.531132	18319.3
$5s\,4d$	$^1D_2$	0.494339	20235	0.522311	20213	0.522792	20149.7
$5s\,6s$	$^3S_1$	0.460940	27566	0.481533	29162	0.482291	29038.8
$5s\,5p$	$^3P^o_0$	0.529636	12489	0.548754	14410	0.549366	14317.5
$5s\,5p$	$^3P^o_1$	0.528850	12662	0.547896	14598	0.548514	14504.4
$5s\,5p$	$^3P^o_2$	0.527213	13021	0.546079	14997	0.546718	14898.6
$5s\,5p$	$^1P^o_1$	0.491616	20833	0.515901	21621	0.515736	21698.5

[a] For the ground state $E_{\rm val}$ = IP (Sr)+IP (Sr$^+$), where IP (Sr) = 45925.6 cm^{-1} and IP (Sr$^+$) = 88964.0 cm^{-1} [39].

TABLE IV: Reduced electric-dipole matrix elements for transitions allowed in LS-coupling. n is the principal quantum number of the first valence s and p shells and m corresponds to the first valence d shell; $n = 3$ for Mg, 4 for Ca, and 5 for Sr; $m = 3$ for Mg and Ca, and 4 for Sr. All values are in a.u.

	Mg		Ca		Sr	
	CI	CI+MBPT	CI	CI+MBPT	CI	CI+MBPT
			$\langle nsnp\,^1P^o_1\|\|D\|\|ns^2\,^1S_0\rangle$			
L-gauge	4.09	4.03	5.20	4.91	5.63	5.28
V-gauge	4.06	4.04	5.11	4.93	5.48	5.32
Final value		4.03(2)		4.91(7)		5.28(9)
Experiment		4.15(10)[a]		4.967(9)[b]		5.57(6)[c]
		4.06(10)[d]		4.99(4)[c]		5.40(8)[e]
		4.12(6)[f]		4.93(11)[g]		
			$\langle nsnp\,^1P^o_1\|\|D\|\|nsmd\,^1D_2\rangle$			
L-gauge	4.43	4.62		1.16	1.75	1.92
V-gauge	4.47	4.59				
Final value		4.62(5)		1.2(3)		1.9(4)
Experiment						1.24(18)[h]

[a] Ref. [5]; [b] Ref. [3]; [c] Ref. [11]; [d] Ref. [12]; [e] Ref. [13]; [f] Ref. [14]; [g] Ref. [15]; [h] Ref. [24].

[19] H. S. Kwong, P. L. Smith, and W. H. Parkinson, Rhys. Rev.A **25**, 2629 (1982).
[20] R. Drozdowski, M. Ignasiuk, J. Kwela, and J. Heldt, Z. Phys. D **41**, 125 (1997).
[21] C. Mitchell, J. Phys. B **8**, 25 (1975).
[22] P. G. Whitkop and J. R. Wiesenfeld, Chem. Phys. Lett. **69**, 457 (1980).
[23] J. F. Kelly, M. Harris, and A. Gallagher, Phys. Rev. A **37**, 2354 (1988).
[24] L. R. Hunter, W. A. Walker, and D. S. Weiss, Phys. Rev. Lett. **56**, 823 (1986).
[25] S.G.Porsev, M.G.Kozlov, and Yu.G.Rakhlina, Pis'ma Zh. Eksp. Theor. Fiz. **72**, 862 (2000)[

TABLE V: Reduced electric-dipole matrix elements for *intercombination* transitions. n is the principal quantum number of the first valence s and p shells and m corresponds to the first valence d shell; $n = 3$ for Mg, 4 for Ca, and 5 for Sr; $m = 3$ for Mg and Ca, and 4 for Sr. All values are in a.u.

	Mg		Ca		Sr	
	CI	CI+MBPT	CI	CI+MBPT	CI	CI+MBPT
$\langle nsnp\,^3P_1^o\vert\vert D\vert\vert ns^2\,^1S_0\rangle$						
L-gauge	0.0055	0.0064	0.027	0.034	0.12	0.16
V-gauge	0.0062	0.0062	0.030	0.032	0.13	0.17
Final value	0.0064(7)		0.034(4)		0.160(15)	
Experiment	0.0053(3)[a]		0.0357(4)[b]		0.1555(16)[c]	
	0.0056(4)[d]		0.0352(10)[e]		0.1510(18)[e]	
	0.0061(10)[f]		0.0357(16)[g]		0.1486(17)[h]	
$\langle nsnp\,^1P_1^o\vert\vert D\vert\vert ns(n+1)s\,^3S_1\rangle$						
L-gauge	0.0088	0.0097	0.035	0.043	0.15	0.19
V-gauge	0.0089	0.0101	0.035	0.045	0.15	0.20
Final value	0.0097(10)		0.043(5)		0.19(2)	
$\langle nsnp\,^3P_1^o\vert\vert D\vert\vert nsmd\,^1D_2\rangle$						
L-gauge	0.0052	0.0049		0.059	0.33	0.19
V-gauge	0.0050	0.0047		0.061	0.36	0.18
Final value	0.0049(5)		0.059(6)		0.19(2)	
$\langle nsnp\,^3P_2^o\vert\vert D\vert\vert nsmd\,^1D_2\rangle$						
L-gauge	0.0039	0.0031		0.028	0.15	0.10
V-gauge	0.0041	0.0032		0.024	0.16	0.06
Final value	0.0031(4)		0.028(3)		0.10(2)	

[a]Ref. [16]; [b]Ref. [17]; [c]Ref. [18]; [d]Ref. [19]; [e]Ref. [20]; [f]Ref. [21]; [g]Ref. [22]; [h]Ref. [23].

JETP Lett., **72**, 595 (2000)].

[26] V. A. Dzuba, V. V. Flambaum, and M. G. Kozlov, Pis'ma Zh. Eksp. Teor. Fiz. **63**, 844 (1996) [JETP Lett. **63**, 882 (1996)]; Phys. Rev. A **54**, 3948 (1996).

[27] V. A. Dzuba, M. G. Kozlov, S. G. Porsev, and V. V. Flambaum, Zh. Eksp. Theor. Fiz. **114**, 1636 (1998) [JETP **87**, 885 (1998)].

[28] T. P. Dinneen, K. R. Vogel, E. Arimondo, J. L.Hall, and A. Gallagher, Phys. Rev. A **59**, 1216 (1999).

[29] T. Kurosu and F. Shimizu, Jpn. J. Appl. Phys., Part 2 **29**, L2127 (1990).

[30] H. Katori, T. Ido, Y. Isoya, and M. Kuwata-Gonokami, Phys. Rev. Lett. **82**, 1116 (1999).

[31] M. Machholm, P. S. Julienne, and K.-A. Suominen, Phys. Rev. A **59**, R4113 (1999);

[32] A. Dalgarno and W. D. Davidson, Adv. At. Mol. Phys. **2**, 1 (1966).

[33] M. G. Kozlov and S. G. Porsev, Opt. Spektrosk. **87**, 384 (1999). [Opt. Spectrosc. **87**, 352 (1999)].

[34] see, for example, D. J. Thouless, *The Quantum Mechanics of Many-Body Systems*, Chapter IV (Academic, New-York, 1975).

[35] S. G. Porsev, Yu. G. Rakhlina, and M. G. Kozlov, J. Phys. B **32**, 1113 (1999).

[36] S. G. Porsev, Yu. G. Rakhlina, and M. G. Kozlov, Phys. Rev. A **60**, 2781 (1999).

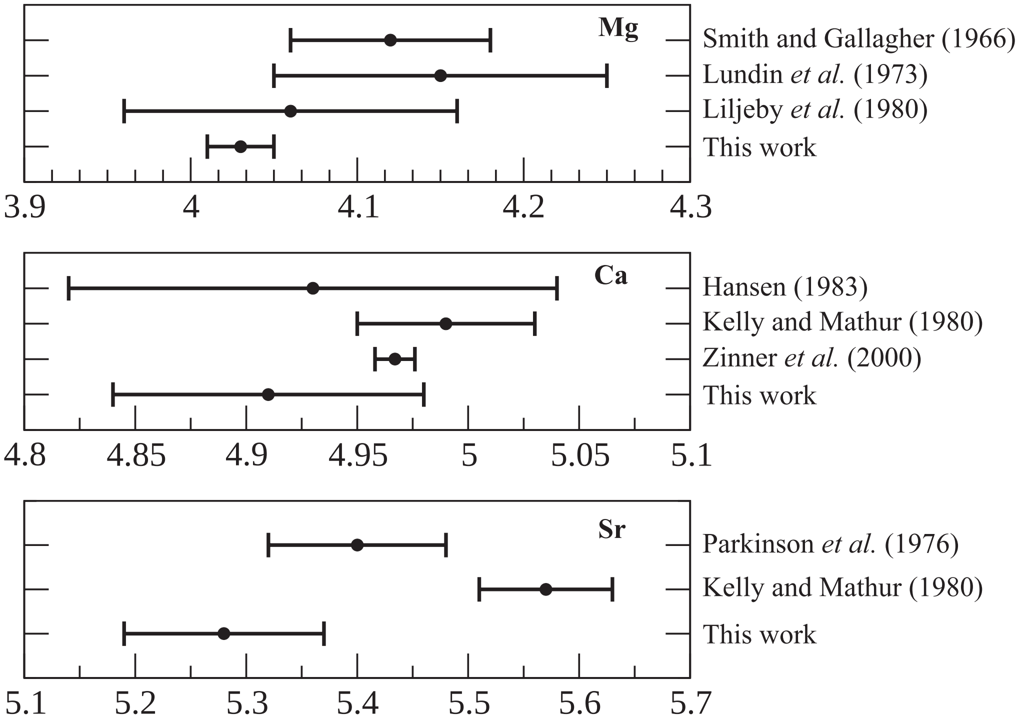

FIG. 1: Comparison of calculated reduced matrix elements $\langle nsnp\,^1P_1^o||D||ns^2\,^1S_0\rangle$ with experimental data in a.u.

[37] Although the calculations were *ab initio* relativistic, for brevity we suppress total angular momentum j in the designations of orbitals.

[38] P. Bogdanovich and G. Žukauskas, Sov. Phys. Collection, **23**, 13 (1983).

[39] C. E. Moore, *Atomic Energy Levels*, Natl. Bur. Stand. (U.S.) Circ. No. 467 (U.S., Washington, 1958).

[40] E. Tiemann, private communication.

[41] C. W. Bauschlicher Jr, S. R. Langhoff, and H. Partridge, J. Phys. B **18**, 1523 (1985).